

Synthesis And Characterization of Zeolite A from Aloji Kaolin Via Hydrothermal Method

ABSTRACT

This study focused on the synthesis and characterization of Zeolite A from Aloji kaolin via the hydrothermal method. The effect of short crystallization times (0.5h, 1h, 1.5h, 2h, and 3h) and high crystallization temperature of 115 °C on the formation of Zeolite A as the final product was investigated. The characterization of the synthesized Zeolite A was conducted using a Scanning electron microscope (SEM), X-ray diffraction (XRD), and Brunauer-Emmett- Teller (BET) analysis. The results showed a well-developed Zeolite A with cubic morphology and a crystallinity of 78.12%, as well as a surface area and pore size of 18.8832 m²/g and 178.461 Å respectively was successfully synthesized using high alkali concentration (5 mol/L) and a crystallization time of 3h. The properties of synthesized zeolite A were found to similar when compared to International Zeolite Association (IZA) standard for commercial zeolite A. The synthesized zeolite is an eco-friendly, renewable, inexpensive and highly efficient for water treatment and adsorption where high surface area and pore volume favors the removal of heavy metals and gases. Thus, the utilization of kaolin for zeolite synthesis will further enhance in exploring sustainable raw materials with the intent of reducing synthesis cost and pollution.

Keywords: [Kaolin, Zeolite, Crystallization, Temperature, Hydrothermal]

1. INTRODUCTION.

The increase in global population as well as rapid industrialization has resulted in the depletion of non-renewable resources, increasing pollution, and thus various ecological and environmental problems. These problems have greatly transcended to the degradation of the environment and human health which has greatly caused people to become inquisitive about the current model of industrialization procedure and production. Due to improvements in regulations and the emergence of new policies, there is a shift in the regular mode of pollution first then treatment later to a cleaner method of production. In the clean production methods harmful and very toxic substances that cause pollution are either avoided or reduced to the barest minimum [1].

Zeolites are microporous, nontoxic, and crystalline aluminosilicate materials that are formed by a three-dimensional network of silica [SiO₄]⁴⁻ and alumina [AlO₄]⁵⁻ tetrahedron having shared oxygen atoms [2-3]. The zeolite's tetrahedral structure comprises a well-organized network of channels, pores, and cavities with molecular dimensions that can be filled with exchangeable cations or water molecules [4-5]. Zeolites commonly referred to as molecular sieves possess uniformly sized pores and find extensive use in diverse applications including catalysis, bacterial adhesion, adsorption processes, water treatment, air pollution control, detergent manufacturing, fuel cells, and ion exchange [3, 6-8].

Zeolites exist in typically two main types namely natural and synthetic. Natural zeolites are mined from sedimentary rocks in the earth whereas synthetic types are manufactured in

35 laboratories. The most common types of natural zeolites include Laumontite, Clinoptilolite,
36 Heulandite, Analcime, Chabazite, and Mordenite [9-10]. These natural zeolites contain various
37 impurities like SO_4^{2-} , Fe^{2+} , SiO_2 , and other zeolites thereby making them unfit for use in fields
38 where uniformity and purity are essential. However, due to the significant demand for zeolite
39 and the expensive nature of purifying natural zeolite, synthetic zeolite materials were
40 developed [3, 11]. Synthetic zeolites are typically favored because of their uniform composition
41 (particle size and shape) and high crystallinity, which surpasses that of natural zeolites. This
42 is primarily because structural properties and chemical compositions can be easily controlled
43 by adjusting synthesis parameters during production [12-13].

44 The preparation and synthesis of synthetic zeolites are highly challenging, and the typical
45 methods of synthesis involve using alumina and silica obtained from analytical/ synthetic
46 chemicals to form aluminosilicate hydrogel which is then crystallized to obtain zeolite. This
47 source of alumina and silica is very expensive and leads to a high cost of zeolite in addition to
48 causing several environmental burdens due to pollution from the use of analytical-grade
49 chemicals [11,14-15]. To eliminate these limitations researchers have been prompted to
50 investigate the synthesis of synthetic zeolite using several other alternative sources such as
51 bauxite [16], clay [17-18], and coal fly ash [19]. Natural clays such as kaolin are readily
52 available, cheap, renewable and abundant when compared to other sources of silica as such
53 they are most frequently used for production of mesoporous silica. Kaolin is an alternative
54 source for alumina and silica because of its low-cost benefit and it has a Si/Al ratio of 1 which
55 is suitable for the synthesis of low silica zeolites. [2,13,20]. Low silica zeolites such as zeolite
56 A, are particularly intriguing because of their exceptional adsorption and ion exchange
57 capabilities [5,21-22]. In general, zeolite synthesis using kaolin as starting material typically
58 involves two stages namely: metakaolinization (the calcination of the raw kaolin at elevated
59 temperature to obtain an amorphous, chemically reactive and stable metakaolin) and
60 hydrothermal treatment of metakaolin with sodium hydroxide [12]. The hydrothermal
61 treatment/method is a conventional method for zeolite synthesis from kaolin. This method is
62 carried out in two main steps: (a) dissolution of meta-kaolin in an alkali solution to form
63 homogenous gel, and (b) crystallization of zeolites in autoclave [18].

64 The hydrothermal synthesis method offers several benefits, including high reagent reactivity,
65 easy control solution, metastable phase formation, and low energy consumption, making it the
66 preferred technique for zeolite synthesis [22]. In this method, elevated alkalinity enhances the
67 solubility of aluminum and silicon sources, reduces silicate anion polymerization, and
68 promotes polysilicate and aluminate anion polymerization. Higher alkalinity during synthesis
69 has been found to shorten induction and nucleation periods while speeding up zeolite
70 crystallization [6]. Optimal crystallization conditions are necessary for specific zeolite phases,
71 as temperature significantly affects nucleation rates and crystal growth, while longer
72 crystallization times enhance crystallinity. However, prolonged crystallization in highly alkaline
73 aluminosilicate gel can lead to the dissolution of zeolite A into sodalite (SOD) [6].

74 Several authors have attempted synthesizing zeolite A from kaolin clay [2,13,16-19]. Ayele et
75 al. [23] successfully synthesized zeolite A using a 3M alkalinity, with a 24-h aging period and
76 crystallization at 100°C for 3 h, achieving 73% crystallinity. Foroughi et al. [20] produced
77 zeolite A from kaolin with a varying NaOH/kaolin weight ratio under similar conditions, resulting
78 in 90% crystallinity. Maia et al. [24] reported successful synthesis from metakaolin using 5M
79 NaOH, 24-h aging, and crystallization at 110°C for 4 h. Nasief et al. [10] synthesized zeolite A
80 from metakaolin at 150°C for 4 h and the obtained zeolite A was used for Ca/Mg ion adsorption
81 from water.

82 In this work, Aloji kaolin was used as an alternative source for alumina and silica because of
83 its low-cost benefit and it has a Si/Al ratio of 1 which is suitable for the synthesis of low silica

84 zeolites. The work involves the synthesis of zeolite A from Aloi kaolin. This will be achieved
85 by refining raw kaolin and then converting this to metakaolin by calcination. The metakaolin
86 will then be used in synthesizing zeolite A.

87

88 **2. MATERIAL AND METHODS**

89

90 **2.1 Materials**

91 Raw Kaolin was obtained from Aloi in Kogi state, Nigeria. The only chemical reagent used
92 was an analytical grade sodium hydroxide (NaOH) pellet of 97% purity obtained from Sigma
93 Aldrich. Also, deionized and distilled water were all obtained from the Laboratory in Chemical
94 Engineering Department of the Federal University of Technology, Minna, and the water was
95 used as received.

96

97 **2.2 Synthesis of Zeolite A**

98 **2.2.1. Refining of kaolin**

99 Zeolite A was synthesized from Aloi Kaolin using the conventional hydrothermal method. Raw
100 Aloi kaolin was crushed mildly and sieved using an 850 μ m sieve mesh. This was then
101 transferred into a 1000ml beaker where it was soaked using deionized water for 12h. The
102 mixture was then stirred continuously for about 30 minutes after which the lighter fraction
103 (supernatant) was collected. After sedimentation, the Kaolin was decanted and dried in the
104 oven.

105 **2.2.2 Preparation of zeolite slurry from metakaolin**

106 The obtained refined Aloi Kaolin was then calcined in a furnace at 850 °C for 2h to obtain
107 metakaolin which is a more reactive form of Kaolin. (amorphous form of kaolin). Zeolite A
108 synthesis requires a Si/Al ratio of approximately 1, since Aloi kaolin has same ratio, it was
109 used without further modification. 5 g of metakaolin was reacted with 50ml of 5.0 M NaOH and
110 the mixture stirred at 700 rpm for 2 h. The resultant homogenous gel obtained was aged for
111 24 h.

112 **2.2.3 Hydrothermal synthesis of Zeolite A**

113 The aged homogenous aluminosilicate gel was heated in a Teflon-lined stainless-steel
114 autoclave at 115 °C for various crystallization times of 0.5 h, 1 h, 1.5 h, 2 h, and 3 h. The
115 resultant product obtained was continuously washed with deionized water to obtain a pH of
116 8.5, after which the synthesized zeolite sample was dried in an oven at 100 °C for 8 h and the
117 zeolite crystals obtained were stored in an air-tight container.

118

119 **2.3 Material Characterization**

120 The Aloi kaolin clay underwent X-ray Fluorescence (XRF) analysis using an XRF-1800
121 Shimadzu, Japan to determine its chemical composition in terms of metal oxides. Additionally,
122 X-ray Diffraction (XRD) analysis was conducted to determine the mineralogical phases and
123 crystalline for the kaolin clay, metakaolin, and synthesized zeolite A using an Ultima IV
124 instrument from Rigaku, UK, utilizing Cu-K α ($\lambda=0.154$) radiation with a fixed power source (40
125 kV, 40 mA). The diffraction angle (2θ) ranged from 5 to 90 degrees. Furthermore, their particle
126 morphologies were examined using high-resolution SEM techniques with a FEI Quanta 400
127 instrument. The surface properties of these materials were investigated through BET analysis
128 using Chem BET 3000, USA.

129

130

131 **3. RESULTS AND DISCUSSION**

132

133 **3.1 X-ray Fluorescence (XRF) for Aloi Kaolin**

134 The XRF analysis of the raw kaolin clay is detailed in Table 1, revealing that Aloji kaolin
 135 primarily comprises 46.42% SiO₂ and 38.76% Al₂O₃. This composition aligns with previous
 136 studies by Dewi et al. [25], Lim et al. [13], and Adeniyi et al. [26], which also found that kaolin
 137 clay predominantly consists of SiO₂ and Al₂O₃. These components, alumina, and silica are
 138 essential constituents for the formation of zeolites. Aloji kaolin exhibits a SiO₂/Al₂O₃ ratio of
 139 1.97 and a Si/Al ratio of 0.98, indicating its suitability for synthesizing zeolite A. Comparatively,
 140 the studies by Lim et al. [13] and Adeniyi et al. [26] reported SiO₂/Al₂O₃ ratios of 2.086 and
 141 1.24 respectively, demonstrating slight variations likely due to differences in the kaolin
 142 sources.

143 **Table 1:** Percentage chemical composition of kaolin based on XRF Analysis
 144

Compound	Value (Wt%)		
	This Work	Lim et al. [13]	Adeniyi et al. [26]
SiO ₂	46.42	45.42	49.20
Al ₂ O ₃	38.76	36.94	39.80
Na ₂ O	1.56	0.00	-
B ₂ O ₃	1.02	-	-
MgO	1.33	0.53	-
K ₂ O	0.52	3.96	0.33
TiO ₂	0.80	0.08	-
Fe ₂ O ₃	3.15	0.36	2.90
FeO	1.25	-	-
MnO	1.17	0.03	0.04
Cr ₂ O ₃	0.05	-	0.04
NiO	0.13	-	0.09
P ₂ O ₅	0.27	0.01	0.36
CaO	1.52	1.68	0.04

145

146 **3.2 XRD ANALYSIS**

147 The XRD pattern for Aloji Kaolin is shown in Figure 1. The pattern shows diffraction peaks at
 148 2θ values of 9.3, 12.66, 21.29, 25.20, 27.0, 36.95, 39.87, and 42.80°. The kaolinite peaks are
 149 evident at 2θ values of 12.66, 25.20, 36.95, and 39.62 while other crystalline phases such as
 150 quartz and mica are found at 2θ values of 21.29 and 27.0°. Similar peaks were reported by
 151 Dewi et al. [25] and Lim et al. [13]. In zeolite synthesis using kaolin, shifts and changes in peak
 152 intensities were mostly observed within the kaolinite peaks, thus indicating that kaolin can be
 153 readily converted into sodium silicate and sodium aluminium silicate, and then finally zeolite.
 154 The metakaolinization process converted crystalline inactive kaolinite to amorphous reactive
 155 metakaolin having only a slight quartz peak as the crystalline phase present.

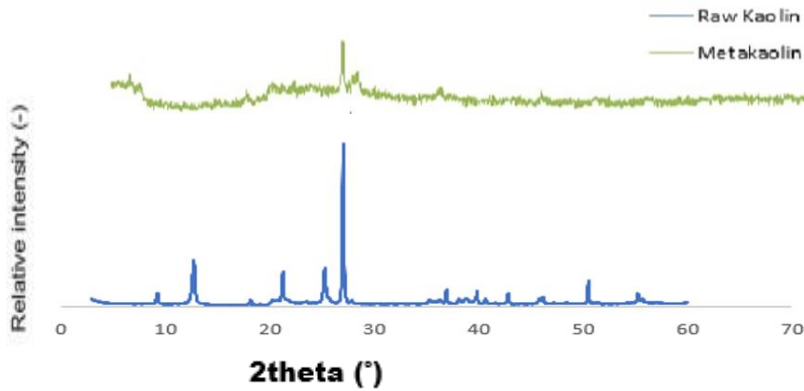


Figure 1. XRD pattern for kaolin and metakaolin

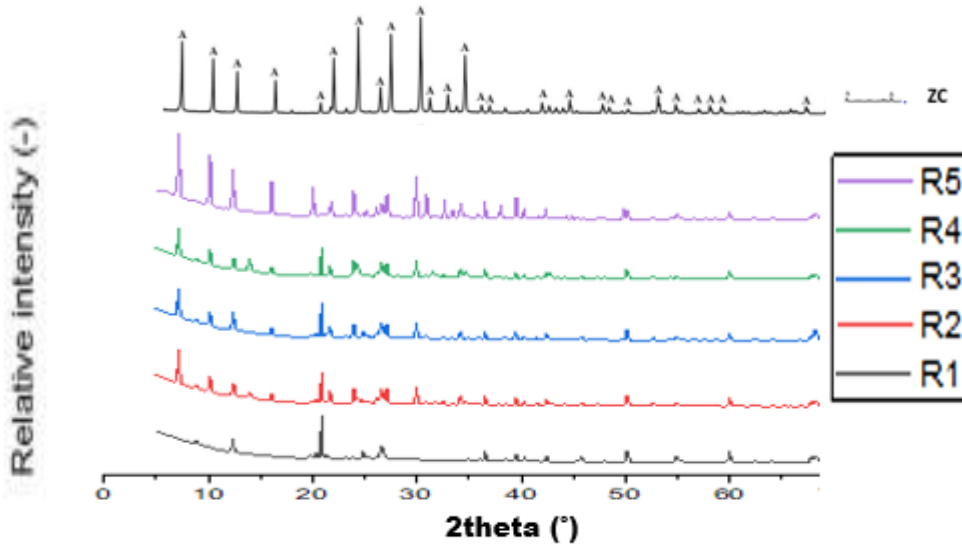


Figure 2. XRD pattern for synthesized zeolite at various crystallization times

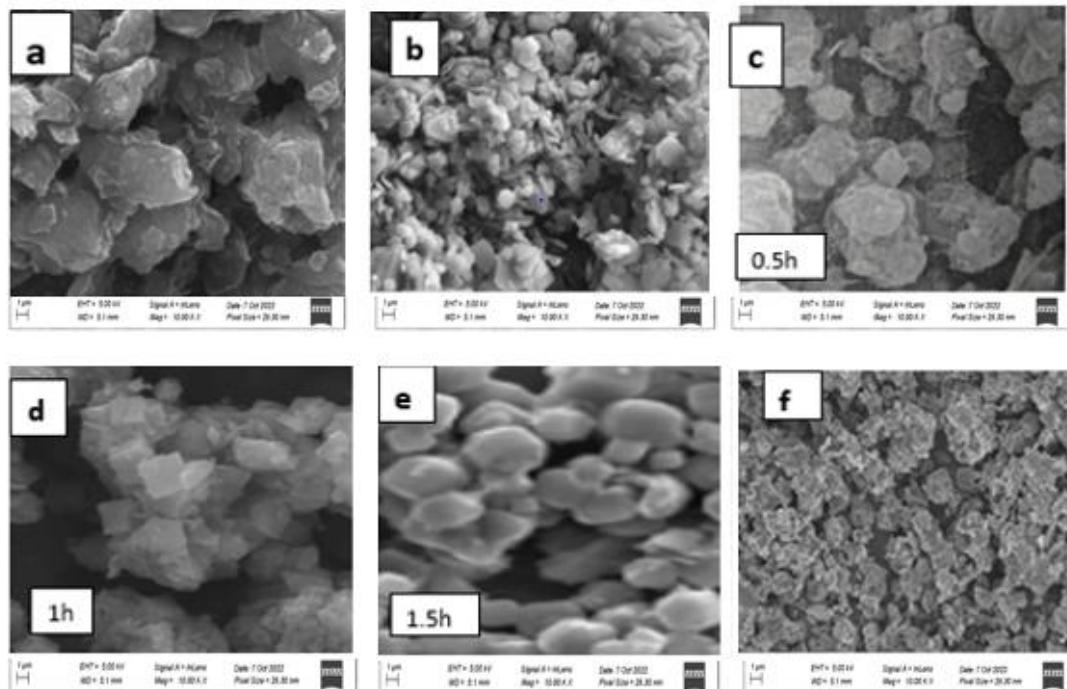
156
157
158
159
160

161
162
163
164

165 In the study of zeolite synthesis, XRD analysis was carried out. Figure 2 shows the XRD
166 pattern for the zeolite synthesized at various crystallization times. It can be seen from the
167 result that the XRD obtained after 0.5 h of crystallization (R1) showed peaks at 2 theta values
168 of 12.51, and 24.64 and quartz peaks at 26.67. However, at a crystallization time of 1 h as
169 indicated by plot R2, other diffraction peaks became visible. Here peaks characteristic of
170 zeolite A (as seen from the XRD pattern of commercial zeolite ZC) began to emerge. The
171 diffraction peaks at 2θ values of 7.18, 10.24, 12.49, 16.04, 20.46, 30.89, and 34.21 were
172 obtained. Similarly, a peak characteristic of faujesite was obtained at a 2θ value of 14.21; this
173 readily disappeared as crystallization time increased to 1.5 h. The diffraction peaks obtained
174 at 1.5 h (R3) have similar peaks as those at 1h. it was observed that more peaks characteristic
175 of zeolite A were added and the faujesite peak disappeared. New peaks that emerged at 1.5
176 h were obtained at 2θ values of 19.98, 24.13, 36.67, 39.65, 42.31 and 42.74. The diffraction
177 peaks obtained after 2 h (R4) crystallization time were seen at 2 theta values of 7.18, 10.24,

178 12.49, 16.04, 20.46, 24.13, 30.89, 34.21, 36.67, 39.65, 42.31, 42.74, 44.25 and 47.34. These
 179 peaks are characteristic peaks obtained for zeolite A according to Tracey and Haggins [27].
 180 This confirms that zeolite A formation begins even after 1h crystallization time and continues
 181 to new peaks emerging with increasing time. Johnson and Arshad [6] in their study revealed
 182 that longer crystallization time produces higher crystallinity. This was observed in this study
 183 as increasing crystallization time resulted in the emergence of more peaks distinct to zeolite
 184 A as well as increased intensity of peaks. The peaks obtained for zeolite synthesized at 3 h in
 185 this study gave the highest crystallinity of 78.12 % and the diffraction peaks were observed at
 186 2θ values of 7.18, 10.24, 12.49, 16.04, 20.46, 21.71, 24.04, 25.15, 30.01, 30.89, 32.68, 34.21,
 187 36.64, 38.04, 39.62, 40.27, 42.38, 44.20, 44.85, and 49.83. These peaks obtained from this
 188 work were in close agreement with that obtained from the works of Yusriadi et al. [27]; Maia
 189 et al. [24] and Vegree et al. [29]. Furthermore, it can be seen from Figure 3.1 that diffraction
 190 peaks obtained from the zeolite crystallized at 3 h had peaks of higher intensities than the
 191 other zeolites synthesized, this may explain the reason for a higher percentage crystallinity
 192 obtained by this zeolite.

193
 194



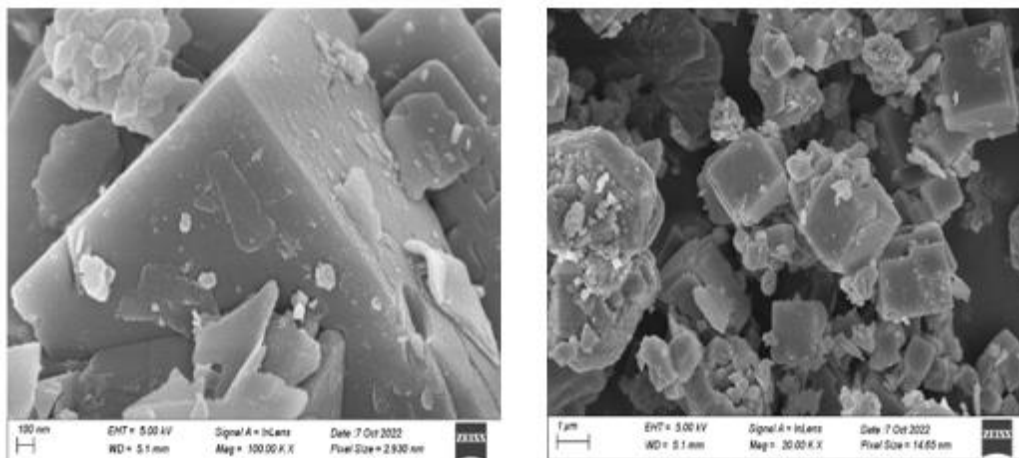
195
 196
 197
 198
 199

Figure 3: SEM images for a) Kaolin b) Metakaolin (c-g) Zeolite A obtained at (0.5-2 h) crystallization times

3.2. SEM ANALYSIS

200 The refined kaolin, metakaolin, and zeolite samples synthesized at various crystallization
 201 temperatures were analyzed using high resolution SEM. The morphologies obtained for each
 202 sample are shown in Figure 3. The micrographs shown in Figure 3a-f give the for the changes
 203 in the morphology of kaolin, metakaolin, and zeolite during synthesis. It was observed from
 204 Figure 3a that the morphology of kaolin is an assemblage of hexagonal plate-like structures
 205 having heterogeneous sizes, while metakaolin also shows flat platted particles having various
 206 sizes. This morphology agrees with the work of Lim et al. [13]

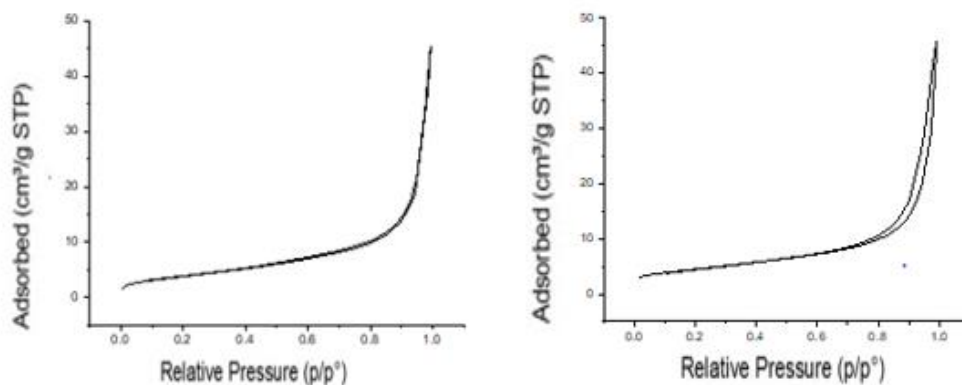
207 The zeolite sample synthesized at various times (0.5-2h) crystallization time is shown in
 208 Figure 3c-f. The micrograph in Figure 3c still depicted dominantly flat plated hexagonal shaped
 209 morphology having some gel-like substance. The micrograph in Figure 3d gives the zeolite
 210 sample formed at 1 h crystallization time. The image shows a mixture of both cubic and
 211 hexagonal-shaped morphology for samples. However, the micrograph also showed an
 212 improvement from the originally flat-plated metakaolin to a transforming cubic shape [30].
 213 Similarly, it agrees with the XRD result that at this crystallization time peaks characteristic of
 214 zeolite were formed, since cubic shaped crystals were observed. Furthermore, in Figure 3e
 215 for 1.5 h crystallization time a similar pattern was identified as samples were seen to contain
 216 crystals of both cubic and hexagonal crystals. In Figure 3f, the micrographs showed crystals
 217 that have predominantly cubic morphology, with very few flat-plated and hexagonal-shaped
 218 crystals present. The XRD result obtained confirms that zeolite samples crystallized for 2 h
 219 produced more peaks that are characteristic of zeolite A than those crystallized at a lesser
 220 time. The micrograph was almost similar to that of the zeolite sample crystallized at 3 h.
 221 Although the sample crystallized at 3h as shown in Figure 4 had better-formed cubes, it still
 222 contained impurities having flat plated morphology that is characteristic of amorphous
 223 metakaolin. This may be the reason for the crystallinity obtained from the XRD result as 100%
 224 crystallinity depict pure zeolite a phase devoid of impurities. This is clearly shown in Figure 4.
 225 The morphology of the synthesized zeolite A after 3 h crystallization time with higher
 226 magnification is shown in Figure 4. The micrograph depicts some well-developed cubic
 227 crystals that are typical of zeolite A. This shape conforms with Kirdeciler and Akata [21] and
 228 Salimkhani et al. [31] who reported obtaining image cubic morphology for zeolite A using kaolin
 229 as the starting raw material.
 230



231
 232 Figure 4: SEM images for zeolite A obtained at 3h crystallization time.
 233

234 **3.3 BET RESULTS**

235 Kaolin and zeolite A synthesized was analyzed to determine the specific surface area, pore
 236 size, and specific pore volume using the Brunauer-Emmett-Teller (BET) method. The BET
 237 adsorption-desorption isotherm for both Alojji kaolin and zeolite A synthesized is shown in
 238 Figure 5. The adsorption isotherm in comparison to International Union of Pure and Applied
 239 Chemistry (IUPAC) classifications corresponds adequately to type IV for both kaolin and
 240 synthesized zeolite A. The curves exhibit an abrupt increase, with a convex shape curve at
 241 the low relative pressure ratios that results from very strong interactions on the silica surfaces.
 242



243
244

Figure 5: The Adsorption-Desorption isotherm for (a) kaolin and (b) zeolite A

245
246

247 The BET results obtained indicate that Aloji kaolin has a surface area, pore size, and specific
248 pore volume values of 14.15 m²/g, 166.593 Å, and 0.001326 cm³/g respectively. However, for
249 the synthesized zeolite A, the BET analysis showed the values of 18.8832 m²/g for surface
250 area, 178.461 Å for pore size, and 0.028064 cm³/g for pore volume. These values represent
251 significant improvements compared to those observed for refined kaolin, highlighting the
252 effectiveness of the synthesis process in enhancing the surface area, pore size, and pore
253 volume of the resulting zeolite A. This outcome is consistent with previous findings by Otieno
254 et al. [14] who reported a surface area of 18 m²/g for zeolite A synthesized from kaolin using
255 a hydrothermal method. Furthermore, the surface area achieved in this study surpasses the
256 values of 11.85 m²/g and 17.39 m²/g reported by Vegere et al. [29] and Jin et al. [22]
257 respectively. However, it is noted that the surface area of the synthesized zeolite A appears
258 lower than the 25.3 m²/g reported by Foroughi et al. [20]. The surface area of a material is
259 closely tied to its porosity, meaning that mesoporous materials typically have a high surface
260 area. Greater mesoporosity enhances a material's adsorption capacity.

261
262

4. CONCLUSION

263 In conclusion, the present study has demonstrated the successful synthesis of zeolite A from
264 Aloji kaolin via hydrothermal method. The effect of varying crystallization times and
265 temperature on the synthesis of zeolite A was investigated, and it was found that a
266 crystallization time of 3 h on an alkali concentration of 5 mol/L resulted in a well-developed
267 zeolite A crystal with high crystallinity and desirable morphological and textural properties. The
268 characterization results obtained through XRD, SEM, and BET analysis confirmed the
269 formation of Zeolite A with a cubic morphology, high surface area, and pore size. These
270 findings suggest that Aloji kaolin can serve as a potential source of raw material for the
271 synthesis of zeolite A which could have potential applications in various fields such as
272 catalysis, separation, and adsorption.

273
274

LIST OF ABBREVIATIONS.

275 SEM: Scanning Electron Microscope
276 XRD: X-ray Diffraction
277 BET: Brunauer- Emmett- Teller
278 XRF: X-ray Fluorescence
279 IZA: International Zeolite Association
280

281

282 **Competing Interest**

283 The authors declare that they have no known competing financial interests or personal
284 relationships that could have appeared to influence the work reported in this paper.

285 **Funding**

286 Not applicable

287

288 **Authors contribution**

289 This work was carried out in collaboration between all authors. Authors VCE and OAP
290 conceptualization, writing of the original draft, writing review & editing. Authors EMG and CAI
291 managed the analyses of the study. All authors read and approved the final manuscript.

292

293 **Conference disclaimer:**

294 Some part of this manuscript was previously presented and published in the conference: 1st
295 faculty of Engineering and Technology conference (FETiCON 2023) dated from 5th – 7th
296 June,2023 in university of Ilorin, Nigeria Web Link of the proceeding:

297 [https://feticon.com.ng/wp-content/uploads/2024/05/PAPER-142-%E2%80%93-SYNTHESIS-
298 AND-CHARACTERIZATION-OF-ZEOLITE-A-FROM.pdf](https://feticon.com.ng/wp-content/uploads/2024/05/PAPER-142-%E2%80%93-SYNTHESIS-AND-CHARACTERIZATION-OF-ZEOLITE-A-FROM.pdf)

299

300 Disclaimer (Artificial intelligence)

301 Option 1:

302 Author(s) hereby declare that NO generative AI technologies such as Large Language
303 Models (ChatGPT, COPILOT, etc.) and text-to-image generators have been used during the
304 writing or editing of this manuscript.

305 Option 2:

306 Author(s) hereby declare that generative AI technologies such as Large Language Models,
307 etc. have been used during the writing or editing of manuscripts. This explanation will
308 include the name, version, model, and source of the generative AI technology and as well as
309 all input prompts provided to the generative AI technology

310 Details of the AI usage are given below:

311 1.

312 2.

313 3.

314

315
316
317
318
319
320
321
322
323
324
325
326
327
328
329
330
331
332
333
334
335
336
337
338
339
340
341
342
343
344
345
346
347
348
349
350
351
352
353
354
355
356
357
358
359
360
361
362
363
364
365
366

REFERENCES

- [1] He, Y., Tang, S., Yin, S., & Li, S. Research progress on green synthesis of various high-purity zeolites from natural material-kaolin. *Journal of Cleaner Production*, 306 (2021) 127248.
- [2] Binay, M.I., Kirdeciler, S.K., & Akata, B. Development of antibacterial powder coatings using single and binary ion-exchanged zeolite A prepared from local kaolin. *Applied Clay Science*, 2019; 182, 1-9. <https://doi.org/10.1016/j.clay.2019.1052>
- [3] Derbe, T., Temesgen, S., and Bitew, M. A Short Review on Synthesis, Characterization, and Applications of Zeolites. *Advances in Materials Science and Engineering*. 2021; <https://doi.org/10.1155/2021/6637898>
- [4] Olaremu, A.G., Odebunmi, E.O., Nwosu, F.O., Adeola, A.O. & Abayomi, T.G. Synthesis of Zeolite from Kaolin Clay from Erusu Akoko Southwestern Nigeria. *Journal for Chemical Society of Nigeria*, 2018; 43 (3), 381-786.
- [5] Kamyab, S. M., & Williams, C. D. Pure zeolite LTJ synthesis from kaolinite under hydrothermal conditions and its ammonium removal efficiency. *Microporous and Mesoporous Materials*. 2021; 318, 111006
- [6] Johnson, E. B. G. & Arshad, S.E. Hydrothermally synthesized zeolites based on kaolinite: A review. *Applied Clay Science*. 2014; 97–98, 215–221
- [7] Albert, A. C., Asadu, C.O., & Abuh, M.A. Synthesis of Zeolite by Thermal Treatment Using Locally Sourced Ugwaka Clay (Black Clay). *Journal of Materials Science Research and Reviews*, 2018; 1 (2), 1-12. DOI: 10.9734/JMSRR/2018/42862
- [8] Hartati, Prasetyoko, D., Mardi Santoso, M., Qoniah, I., Leaw, W. L., Firda, P. B. D., and Nur, H. A review on synthesis of kaolin-based zeolite and the effect of impurities. *Journal of the Chinese Chemical Society*. 2020; 1–26.
- [9] Tasić, Z.Z., Bogdanović, G.D., & Antonijević, M.M. Application of Natural Zeolite in Wastewater Treatment –A Review. *Journal of Mining and Metallurgy*. 2019; 55 A (1) 67-79. doi: 10.5937/JMMA1901067T
- [10] Nasief, F.M., Shaban, M., Alamry, K.A., Abu Khadra, M.R., Khan, A.A.P., Asiri, A.M., & Abd El-Salam, H.M. Hydrothermal synthesis and mechanically activated zeolite material for utilizing the removal of Ca/Mg from aqueous and raw groundwater. *Journal of Environmental Chemical Engineering*, 2021; 9, 105834
- [11] Yoldi, M., Fuentes-Ordóñez, E.G., Korili, S.A., & Gil, A. Zeolite synthesis from industrial wastes. *Microporous and Mesoporous Materials*, 2019; 287, pp 183–191.
- [12] Aragaw, T. A., & Ayalew, A. A. Removal of water hardness using zeolite synthesized from Ethiopian kaolin by hydrothermal method. *Water Practice & Technology*, 2019; 14 (1), 145-159. doi: 10.2166/wpt.2018.116.
- [13] Lim, W., Lee, C., & Hamm. S. Synthesis and characteristics of Na-A zeolite from natural kaolin in Korea. *Materials Chemistry and Physics*, 2021; 261, 124230

- 367 [14] Otieno, S.O., Kengara, F.O., Kemmegne-Mbougouen, J.C., Langmi, H.W., Kowenje,
368 C.B.O., & Mokaya, R. The effects of metakaolinization and fused-metakaolinization
369 on zeolites synthesized from quartz-rich natural clays. *Microporous and Mesoporous*
370 *Materials*, 2019; 290, 109668
371
- 372 [15] Kumar, M.M & Jena, H. Direct single-step synthesis of phase pure zeolite Na–P1,
373 hydroxy sodalite, and analcime from coal fly ash and assessment of their Cs+ and
374 Sr2+
375 removal efficiencies. *Microporous and Mesoporous Materials*, 2022; 333, 111738.
376
- 377 [16] Rahman, A., Ur Rehman, W., Khan, F.U., & Shah. J. Synthesis of Zeolite 4A Using
378 Bauxite as Aluminum Source: Characterization and Performance. *Journal of Chemical*
379 *Technology and Metallurgy*, 2021; 56, 2, 327-330.
380
- 381 [17] Srilai, S., Tanwongwan, W., Onpetch, K., Wongkitikun, T., Panpiemrasda, K.,
382 Panomsuwan, G., & Eiad-ua, A. *Synthesis of zeolite A from bentonite via*
383 *hydrothermal method: The case of different base solution*. The Second Materials
384 Research Society of Thailand International Conference AIP Conference Proceedings
385 2279, 2020; 060006-1–060006-6; <https://doi.org/10.1063/5.0025043>
386
- 387 [18] Arasi, M. A., Salem, A., & Salem, S. Production of Mesoporous and Thermally Stable
388 Silica Powder from Low Grade Kaolin Based on Eco-Friendly Template free Route via
389 Acidification of Appropriate Zeolite Compound for Removal of Cationic Dye from
390 Wastewater. *Sustainable Chemistry and Pharmacy* 2021; 19, 1-10.
391 <https://doi.org/10.1016/j.scp.2020.100366>
392
- 393 [19] Yang L, Qian X, Yuan P, Bai H, Miki T, Men F, Li H, & Nagasaka T. Green synthesis
394 of zeolite 4A using fly ash fused with synergism of NaOH and Na₂CO₃. *Journal of*
395 *Cleaner Production*, 2019; doi: <https://doi.org/10.1016/j.jclepro.2018.11.259>.
396
- 397 [20] Foroughi, M., Salema, A., & Salem, S. Characterization of phase transformation from
398 low grade kaolin to zeolite LTA in fusion technique: Focus on quartz melting and
399 crystallization in presence of NaAlO₂, *Materials Chemistry and Physics*, 2021; 258, 1-
400 9. <https://doi.org/10.1016/j.matchemphys.2020.123892>
401
- 402 [21] Kirdeciler, S. K. & Akata, B. One pot fusion route for the synthesis of zeolite 4A using
403 kaolin. *Advanced Powder Technology*, 2020; 31, 4336–4343.
404 <https://doi.org/10.1016/j.appt.2020.09.012>
405
- 406 [22] Jin, Y., Li, L., Liu, Z., Zhu, S., & Wang, D. Synthesis and characterization of low-cost
407 zeolite NaA from coal gangue by hydrothermal method. *Advanced Powder*
408 *Technology*, 2021; 32, 791–801. <https://doi.org/10.1016/j.appt.2021.01.024>
409
- 410 [23] Ayele, L., Perez-Pariente, J., Chebude, Y., & Díaz, I. (2016). Conventional versus
411 alkali fusion synthesis of zeolite A from low grade kaolin. *Applied Clay Science*, 132,
412 485–490. <http://dx.doi.org/10.1016/j.clay.2016.07.019>
413
- 414 [24] Maia, A. B., Dias, R. N., Rômulo, S. A., and Neves, R.F. Influence of an aging step on
415 the synthesis of zeolite NaA from Brazilian Amazon kaolin waste. *Journal of Material*
416 *Research and Technology*; 2019; 8(3):2924–2929
417

- 418 [25] Dewi, R., Agusnar, H., Alfian, Z., & Tamrin. Characterization of technical kaolin using
419 XRF, SEM, XRD, FTIR and its potentials as industrial raw materials *Journal of*
420 *Physics: Conference Series*, 2018; 1116, 1-7. doi:10.1088/1742-
421 6596/1116/4/042010.
422
- 423 [26] Adeniyi, F. I., Ogundiran, M. B., T. Hemalatha, T., & Hanumantrai, B. B.
424 Characterization of raw and thermally treated Nigerian kaolinite-containing clays
425 using instrumental techniques *Springer Nature Applied Sci*, 2020; 2, 821-829
426 <https://doi.org/10.1007/s42452-020-2610-x>
427
- 428 [27] Treacy, M.M.J & Higgins, J.B. Collection of simulated XRD powder patterns of
429 zeolites. Fourth revised edition, *Amsterdam Elsevier*. 2001; 379
430
- 431 [28] Yusriadi, Y., Sulastri, E., & Lembang, N. Synthesis of Type A Zeolite from Rice
432 Husk Ash and Its Application as a Builder on Effervescent Tablet Form Detergent.
433 *Tenside Surfantant Detergent*, 2020; 57, 3.
434
- 435 [29] Vegree, K., Kravcevic, R., Krauklis, A.E., & Juhna, T. Comparative study of
436 hydrothermal synthesis routes of zeolite A. *Materials Today: Proceedings*, 2020;
437 <https://doi.org/10.1016/j.matpr.2020.06.326>
438
439
- 440 [30] Gougazeh, M & Buhl, J. Synthesis and characterization of zeolite A by the
441 hydrothermal transformation of natural Jordanian kaolin. *Journal of the*
442 *Association of Arab Universities for Basic and Applied Sciences*. 2014; 15,
443 pp.35–42
444
- 445 [31] Salimkhani, S., Siahcheshm, K., Kadkhodaie, A., & Salimkhani, H. Structural analysis
446 and the effect of the chromium on LTA (Na) zeolite synthesized from kaolin. *Materials*
447 *Chemistry and Physics*, 2021; 271, 124957.
448
449

